Understanding the Cathode-Electrolyte Interphase in Lithium-Ion Batteries

Sungjemmenla,[1] S. K. Vineeth,[1,2] Chhail Bihari Soni,[1] Vipin Kumar,[1,2] Zhi Wei Seh[3*]*

[1] Department of Energy Science and Engineering, Indian Institute of Technology Delhi, Hauz Khas, New Delhi, India 110016

[2] University of Queensland- IIT Delhi Academy of Research (UQIDAR), Indian Institute of Technology Delhi, Hauz Khas, New Delhi, India 110016

*[3] Institute of Materials Research and Engineering, Agency for Science, Technology and Research (A*STAR), 2 Fusionopolis Way, Innovis, Singapore 138634*

[*]Correspondence: vkumar@ces.iitd.ac.in (Vipin Kumar); sehzw@imre.a-star.edu.sg (Zhi Wei Seh)

Abstract

The electrode-electrolyte interface is one of the major components enabling Li-ion batteries (LIBs) to function reversibly. Often, the solid-electrolyte interphase (SEI) at the anode is regarded as the key interface that determines the cycle life, capacity fade, and overall safety of batteries. There are a plethora of SEI literatures that exist, however, the cathode-electrolyte interphase (CEI) remains relatively unexplored. Unlike in the case of SEI, we lack a detailed understanding of CEI formation and its association with battery performance. This review gives insight into the recent progress in understanding the CEI in LIBs. Though there is a relative dearth of literature, the CEI is generally considered as a heterogeneous multicomponent film formed due to the decomposition of electrolyte at the cathode surface. Besides understanding the thermodynamic properties and relevant kinetic reactions, one of the main challenges lies in developing and stabilizing the CEI layer due to its complex structural composition. Extensive research efforts to engineer a stable CEI are reviewed, including the use of electrolyte additives, artificial engineering and heteroatom doping of cathode. Furthermore, we highlight promising characterization techniques and future outlook in forming a robust CEI for both existing LIB and post-LIB systems.

Keywords

Lithium-ion battery; cathode-electrolyte interphase, solid-electrolyte interphase; electrolyte additives; dopants; characterization

1. Introduction

Since the evolution of high-energy rechargeable battery technologies, Li-ion batteries (LIBs) have revolutionized the electronic market with state-of-the-art designs in the portable and mobile sectors.[1–3] Considering the extreme operating potentials of anode and cathode, new solid phases are formed at the electrode-electrolyte interface (EEI).[4] The EEI is represented as a 2D boundary, having a thickness of less than 1 nm, between the surface of the electrode and the counter ions of the electrolyte.[5] As the electrode material and electrolyte molecules interact during initial electrochemical processes, it can catalyze electrolyte degradation.[6] Chemically the degradation products are inorganic and organic derivatives of lithium formed at the EEI.[7,8] The cycling process further contributes to the electrolyte degradation and leads to a continuous layer or film, which further passivates the electrodes. The thickness of the continuous layer is technically in the range of few nanometres to micrometers, and it can be viewed as a 3D interphase instead of a 2D interface.[9] With the application of high voltage at the cathode, a series of degradation mechanisms occur at the cathode-electrolyte interphase (CEI).[10] For instance, dissolution of metal ions from the cathode into the electrolyte and oxygen evolution reaction can occur that lead to overall failure of LIBs,[11] warranting a more detailed understanding of the CEI.[12]

An ideal CEI should be electronically insulating while providing a conductive pathway for Li^+ ion transport to ensure high electrochemical performance.[7] Attempts have been made to unveil the formation mechanism of CEI, and some progress has been made to study the structure and composition of the interface.[13,14] Nevertheless, unlike the solid-electrolyte interphase (SEI) at the anode, the CEI remains poorly investigated and understood to date.[15] In fact, there are still controversies in the literature regarding the morphology and properties of the CEI, which may be due to its nanoscale dimension, complex chemical nature, and extreme air/beam sensitivity.[16] The experimental and theoretical elucidation of the CEI can be complex; its mechanism, transport properties, and structure are still under debate.[5] In particular, identifying the actual composition of chemical species on the CEI and its structural characterization can be challenging under *in-situ*/operando conditions.[17]

Therefore, the aim of this review is to shed light on the complexity of CEI formation in LIBs. We will first discuss how a typical CEI is formed, followed by recent research trends in the development of a stable CEI through electrolyte additives, artificial engineering and heteroatom doping of cathode. In addition, we also highlight promising characterization techniques and propose potential future studies that can be done to further understand and engineer the CEI. It is envisioned that a critical understanding of how to modify and engineer a robust CEI will inspire the development of efficient LIBs.

2. Formation and modification of the CEI

The efficiency and performance of LIBs require localized engineering of the electrolyte and electrodes, which essentially facilitate Li-ion transport throughout the cell.[18–20] Interfacial resistances at the EEI are developed due to the parasitic reaction between electrodes and electrolyte forming a complex heterogeneous mixture of organic and inorganic compounds.[21,22] Intimate contact between electrode and electrolyte results in a series of side reactions which contributes to irreversibility, capacity loss and hence shortens the lifespan.[23] The parasitic side reactions are acid-base reactions, nucleophilic reactions, dissolution of active material, polymerization reactions, and others.[24,25]

The formation of CEI occurs as a result of electrolyte decomposition on the cathode surface. For instance, the nucleophilic cathodic materials, which show Lewis basicity, can coordinate to oxygen atoms from electrolyte species and start a redox reaction.[13] Oxidation/reduction of electrolyte species can be engineered based on the redox potential of the electrodes and the oxidation/reduction potentials of the electrolyte. If the Fermi energy of the cathode is lower than the highest occupied molecular orbital (HOMO) of the electrolyte, electrolyte species are prone to get oxidized.[26,27] Electrolyte reduction occurs when the Fermi energy of the anode is higher than the lowest unoccupied molecular orbital (LUMO).[28,29] The CEI and SEI will be formed when the applied potential exceeds the electrochemical stability window of the electrolyte.[30] Engineering the stability and thickness of CEI can mitigate the consumption of transition metal ions of cathode and prevent further corrosion by electrolyte reaction.[31] **Figure 1** illustrates the schematic of the interfaces in a LIB, where the CEI is represented as a thick region made of complex mixture of different components.

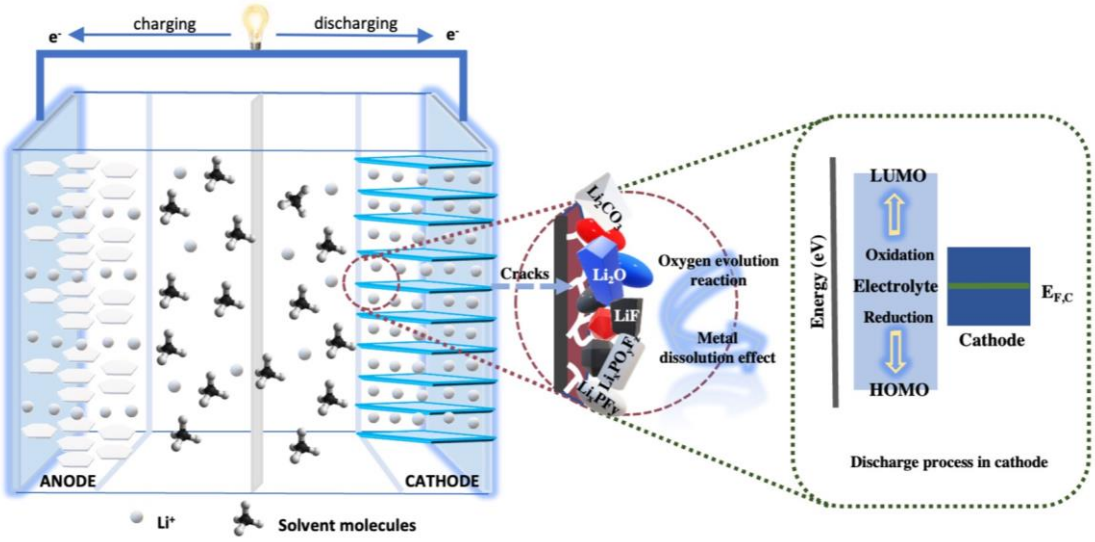

Figure 1. Schematic representation of the formation of CEI in a typical LIB. The formation of the CEI is subjected to the chemical potential of the cathode materials and nature of the electrolyte solvent, salt and other additive species.

i) Electrolyte additives to tune the CEI

Multiple efforts have been made to construct a suitable electrode/electrolyte system to form robust interfaces.[32,33] Despite their efforts, stabilization of CEI requires intensive efforts due to the close contact between electrolyte and cathode, leading to oxidative electrolyte decomposition and complex parasitic mechanisms. One of the major bottlenecks to achieving an optimized CEI is the undesirable side reactions at the interface, e.g., oxygen evolution reactions.[34] Additives (e.g., salt or solvents) have been used to alter and mitigate the deterioration of the interface.[35,36] The additives must have a lower oxidative potential than carbonate-based electrolytes so that the oxidation of the additives occurs on the electrode first before the solvent molecules.[37] Addition of electrolyte additives can result in a uniform and stable CEI with a more robust interface structure on the cathode, enhancing overall electrochemical performance.[38]

A rational design of different functional electrolyte additives has been examined to monitor changes in the CEI's properties. This is supported by a study based on the additives of 3-hexylthiopene (3HT) and lithium difluoro(oxalate)borate (LiDFOB).[39] The careful balance between the additives and the solvent enabled a direct reduction in the catalytic degradation of the solvent. The additives also protected the transition metal oxide cathodes from harmful

reactions as the oxidation of additives on the surface of the cathode could behave as a "corrosion inhibitor film", resulting in the prevention of attack and passivation from protons. With the addition of 2 wt.% trimethyl borate (TMB) with higher oxidation activity to the baseline electrolyte, a thin uniform film was preferentially formed on the cathode surface.[40] The electrophilic layer of boron substrate on the CEI successfully captured the superoxide anion species and improved the structural stability and performance of the electrode. Another similar boron-containing composite could be effectively used as an additive, where methylboronic acid MIDA ester (ADM) with 1 wt.% boron-nitrogen-oxygen alkyl groups delivered a high capacity retention and rate capability.[41] The structural fluctuations could be buffered during the continuous cycling process due to smooth interface film constituting B-O, B-F, $Li_xPO_yF_z$ components. As illustrated in **Figure 2a,** a relatively smooth and consistent film could be formed to prevent further reduction of electrolytes, as supported by their stable electrochemical performance over 25 cycles, which can be improved in future studies.

Recent studies claim that the metal-ion solvation/de-solvation process can affect the dynamics of EEI during continuous interactions among ion and solvent molecules.[28] Therefore, with further modification of the electrolyte additives' molecular structure and electron affinity properties, their influence on interface reactions, electrolyte deterioration, and solvation process can be optimized (see **Figure 2b**).[42] A high voltage across the electrodes often results in degradation of the cathode and the interface. However, a recent study applied a multifunctional methoxytriethyleneoxy-propyltrimethoxysilane (MTE-TMS) additive to stabilize a Ni-rich NCM cathode.[43] Owing to the formation of a protective film comprising Si species, the cell retained a long-term cycling performance even at a high voltage without affecting the physical nature of the interface and dissolution of the transition metal ions. Compared to the standard electrolyte, the higher oxidation activity of MTE-TMS alleviated further electrolyte decomposition, decreased polarization effect and enhanced reversibility during the intercalation-deintercalation process. Additionally, the cathode cycled with MTE-TMS additive showed mostly organic components covering the decomposition products, resulting in a uniform and thin surface film. The formation of a thin CEI layer could enhance the capacity retention, which may result from lower interfacial impedance and a slower decomposition process at a higher voltage range.

ii) Formation of an artificial CEI

The formation of an artificial CEI layer by a protective coating has been shown to enhance the cycling performance when applied at high potentials.[44–47] Some coatings include, but are not limited to, phosphates ($AlPO_4$,[48–51]) oxides (ZrO_2,[50] TiO_2,[52] Al_2O_3,[53]), fluorides (AlF_3,[54]) and others. Application of coating materials to the surface of transition metal oxide cathodes involves: i) modification of interlayer to provide an effective suppression towards metal dissolution and ii) further reduction of surface reaction between the active material and the electrolyte to minimize decomposition of active materials and stabilize the CEI.[55,56] However, how does the uniformity, compactness and thickness of the coating layer affect the capacity retention upon cycling? These unresolved questions have led to discrepancies in the working mechanism of the interlayer and restricted the optimization of various electrodes. Understanding the fundamental influence of coating on the electrode material and its structural fluctuations and composition, can allow for tuning the performance of surface-modified cathodes.

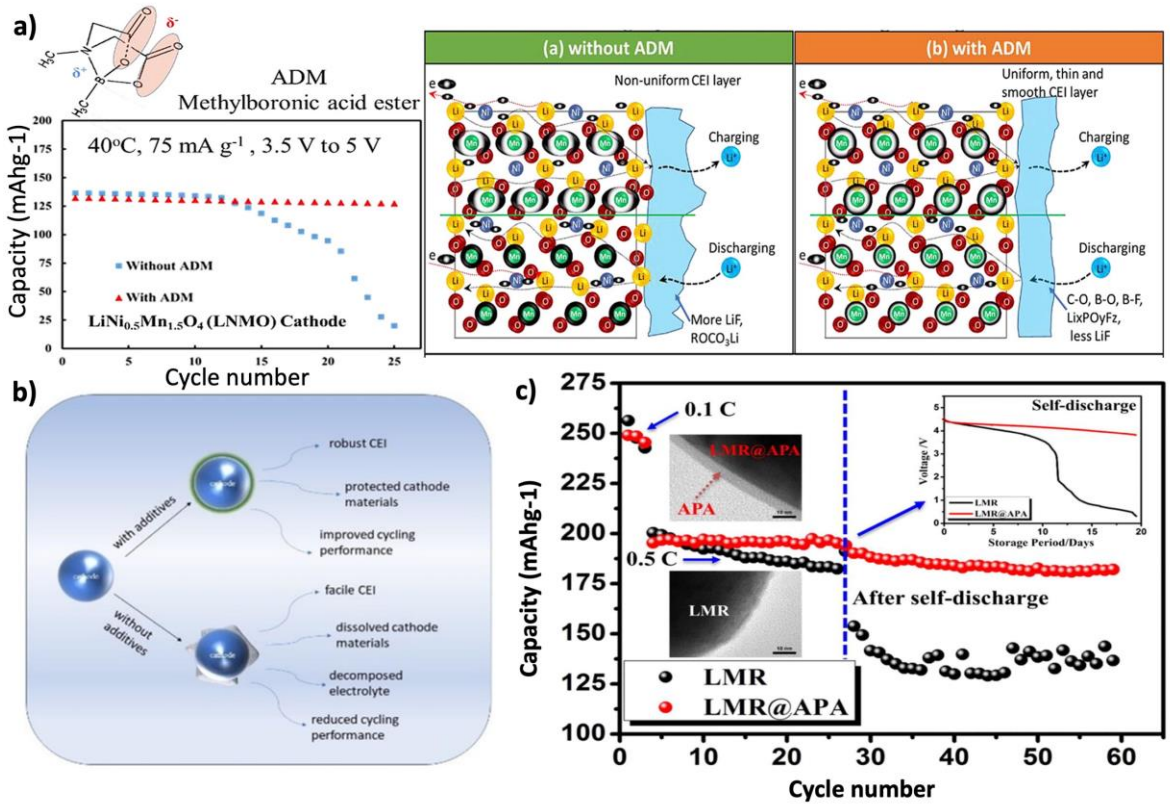

Figure 2. (a) Schematic illustration of atomic environment and Li^+ and e- transfer performance on the interface with and without ADM additive. Reproduced with permission.[41] Copyright 2020, Elsevier. (b) Schematic diagram of influence of additives on the stability of the CEI. Reproduced with permission.[42] Copyright 2020, Wiley. (c) Cycling performance of LMR and

LMR@APA cathodes with their self-discharge profiles. Reproduced with permission.[57] Copyright 2021, Elsevier.

Efforts have been made in modifying the cathode surface, such as matching a lithium/manganese-rich oxide layered $Li_{1.2}Mn_{0.55}Ni_{0.15}Co_{0.1}O_2$ (LMR) cathode with aromatic polyamide (APA).[57] High interfacial stability could be achieved for the high voltage cathode via a robust interface of 5 mm thickness. It should be noted that due to the high solubility of APA in the carbonate-based electrolyte, there could have been a possible strong interactive force with the transition metal ions on the electrode, resulting in suppressed dissolution of metal ions and electrolyte oxidation reactions. The protective interface formed via the coating approach suppressed the parasitic reactions and significantly improved the storage and cyclic performances, as depicted in **Figure 2c**. The cell's performance with and without APA was investigated at 0.5 C, and after some 25 cycles at 4.8 V, the cells were left for a storage period of 20 days. The superior interface stability of the cathodes with APA was further demonstrated over 60 cycles, compared to a huge decay in capacity and voltage for the case without APA.

Likewise, a phosphate coated layer of $AlPO_4$ on $LiCoO_2$ electrodes showed surface components of LiF and $Li_xPF_yO_z$ with a considerable increase during the cycling process, depicting a partial coverage of Li_xCoO_2 electrodes.[58] On further increasing the cycle life, a good amount of Co-and Al-containing fluorides or oxyfluorides with additional $PF_x(OH)_y$ species were developed and completely covered the surface of Li_xCoO_2. Interestingly, scanning electron microscope (SEM) images in **Figure 3a-d** revealed a relatively smooth electrode layer even after 20 cycles; however, additional deposition of components could be observed on the surface of the coated cathodes. The deposition layer enabled the growth of a low impedance region, which leads to enhanced capacity. This may be due to the lower dissolution effect of Co-species from the positive coated electrodes during cycling and controlled deposition on the negative electrode. In addition, the cycled coated-electrodes promoted the formation of Co-Al-O-F species, which could further reduce electrolyte degradation on the active components and possibly prevent the loss of bulk oxygen. Upon subsequent cycling, the coating interlayer could alleviate the growth of highly insulating and resisting films, endowing high stability to the coated electrodes.

iii) Heteroatom doping of cathode to tune the CEI

It is a known fact that the build-up of an interface layer can protect against electrolyte and cathode degradation process.[59] Nevertheless, the coating components may fail to align with the host component's surface lattice structure, resulting in the formation of a less compact CEI layer, which accounts for dissolution effect and degradation of the cathode. One successful approach that has been reported to alleviate this issue is elemental doping that could stabilize the structure and augment the ion/electron charge transfer.[60–63] Aluminum (Al), as a dopant, could be utilized to improve the thermal and structural stability of the CEI.[64–66] The cathode comprising metal-oxide lattice, such as Ni- and Co-rich phases was chemically modified with Al to augment the battery performance.[67] The kinetic redox reactions may form a protective barrier of Al-F or Al-O-F layer at the oxide cathodes interface, thus breaking the bridge between cathode and electrolyte. Based on different electrolyte salt systems, different concentrations of Al can form stable CEI layers.

Similarly, a unique approach of dilute lattice doping of Al in Ni-rich cathode oxides (NCA) could modify the interfacial reactions for improved battery performance.[68] This can be attributed to the partial dissolution of trace amounts of Al in the interface's bulk lattice structure, which could lead to the existence of aluminum oxide nano-islands enriched on the primary particle surface. These aluminum species dressed on the film's surface could successfully lower the redox reaction energy of transition metal oxides, promoting the formation of a stable CEI layer. SEM images are depicted in **Figure 3**, where the secondary particle morphology and evolution of interface structure could be observed. The bare cathode has been observed with severe disintegration during the cycling test, with a large number of inter-granular cracks nucleating from the periphery towards the center (see **Figure 3e, g**). On the contrary, the doped NCA cathode was featured with minimized disintegration and cracks, which indicates the alleviated pulverization effect due to the presence of Al-dopant (see **Figure 3f, h**). Scanning transmission electron microscopy (STEM) observations coupled with energy-dispersive X-ray spectroscopy (EDS) mappings revealed the presence of phosphorus-rich CEI from the decomposition of $LiPF_6$, as supported by atomistic simulations. Thus, the coupled layers of interface and Al_2O_3 nano-islands could lead to the development of a phosphate-containing CEI layer and further inhibit the damage of the cathode.

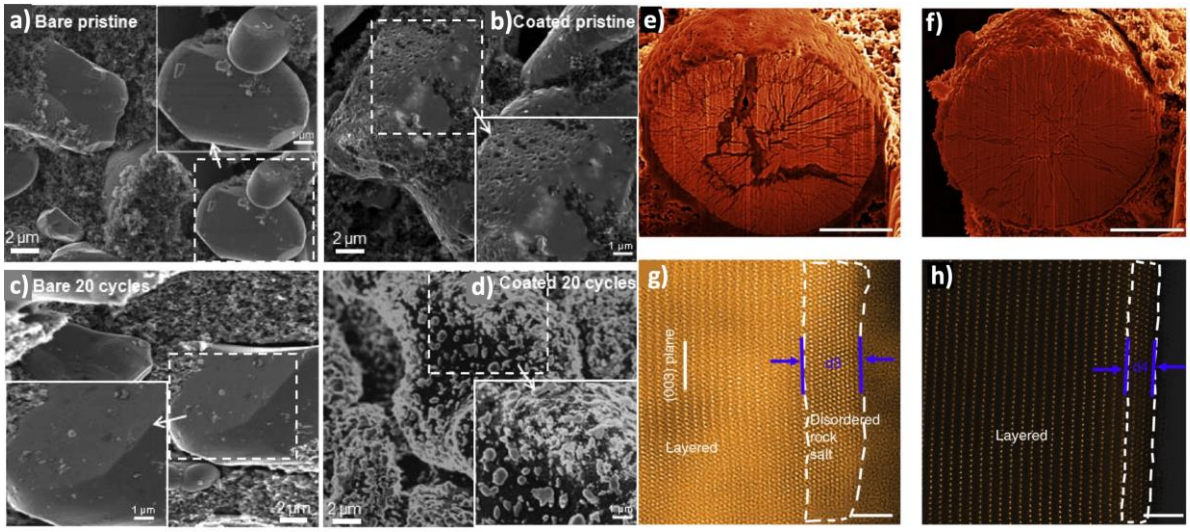

Figure 3. SEM images of (a) bare $LiCoO_2$, (b) $AlPO_4$-coated $LiCoO_2$, (c) bare $LiCoO_2$ after 20 cycles to 4.7 V, (d) $AlPO_4$-coated $LiCoO_2$ after 20 cycles to 4.7 V. Reproduced with permission.[58] Copyright 2009, American Chemical Society. SEM images of (e) NC and (f) NCA cathodes from a cross-sectional view, depicting the secondary particle pulverization after 100 cycles. Phase transition on (g) NC and (h) NCA surfaces. Reproduced with permission.[68] Copyright 2019, Springer Nature.

A new concept of co-doping of zirconium and aluminum in the cathode materials has become apparent to enhance the characteristics at the atomic scale.[69] Zr^{4+}/Al^{3+} co-doped material in a nickel-rich $LiNi_{0.83}Co_{0.11}Mn_{0.06}O_2$ cathode induced a stable shell on the doped layer of the cathode composite. Effective stabilization of the internal morphology of the film with reduced interfacial parasitic reactions and phase transformation was achieved as a result of the co-doping synergistic effect. These studies suggest the further regulation of lattice structure and interface compositions for designing a stable interface film for transition metal layered cathodes.

3. Characterization techniques

Electrochemical characterization tools such as impedance analysis came into view to study various intercalated systems, for instance, $Li_{1-x}CoO_2$.[70] Time-dependent AC impedance spectroscopy is often deployed to examine the controlled diffusion of the interlayer. Consistent with the surface-layer models, a polymeric film on the surface of $Li_{1-x}CoO_2$ could allow the trapping of ions within the electrode. Despite that, no direct information on the components and compositions of the layer could be determined. The cathodes' stabilization may be

considered one of the key points to achieve a stable passivation film that can prevent further interaction between the lithiated species and the electrolyte solution. Various electrochemical techniques, such as slow scan-rate cyclic voltammetry, electrochemical impedance spectroscopy, potentiostatic intermittent titration technique, and chrono-potentiometry have been conducted to investigate the electroanalytical behavior of the electrodes. The spectral studies show the formation of the Li_2CO_3 layer on the LMO electrode, which may be attributed to the mechanistic reaction between $LiMO_x$ species with CO_2 present in the atmosphere, resulting in surface species of $ROCO_2Li$ on prolonged cycling. Upon application of higher potential, it may promote decomposition of the solution species and result in surface film formation on the cathode.

An in-depth study of interfacial mechanisms and the underlying influence of EEI on the electrochemical performance of LIBs has become necessary. This subject relates to a heterogeneous interface layer's composition analysis and formation mechanism, as studied using *in-situ* scanning electrochemical microscopy (SECM).[71] Combining degradation of $LiMn_2O_4$ in contact with the electrolyte and the fluoride species' reactions results in unique $–(CF)_n–$ bonds besides Li_2CO_3, LiF, and MnF_2. The as-formed CEI amorphous layer was discontinuous and not completely insulating for electrons, which can be attributed to the loosely packed $–(CF)_n–$ bonded layers and irreversibility of Li residuals, resulting in increased conductivity. The conductive CEI layer could have protected the cathode surface, provided interface heterogeneity evolvement during cycling, and alleviated the fading rate. The Mn dissolution phenomena in a $LiMn_xO_y$ electrode and the resultant performance of complex Mn species in the interface could be significantly influenced by the presence of different salts of Li anions in the electrolyte system (ClO_4^-, PF_6^-, and $(CF_3SO_2)_2N^-$). Oxygen evolution reactions and the metal dissolution process occurring at CEI can be considered roadblocks in developing a battery with a long cycle life.[72] Using a combination of *in-situ* and *ex-situ* characterization techniques, quantification and monitoring of metal dissolution and oxidative nature of evolved transition metal products can be used to study the degradation species of a thin film $LiMn_xO_y$ cathode as a function of electrolyte's composition.[73] Accelerated dissolution of Mn species could be observed in ClO_4^-, PF_6^- in the electrolyte systems due to disproportionation reactions (see **Figure 4a**). This may be likely due to the oxidative reactions followed by the generation of HF or HCl acids, resulting in an electrochemically unstable system.[73]

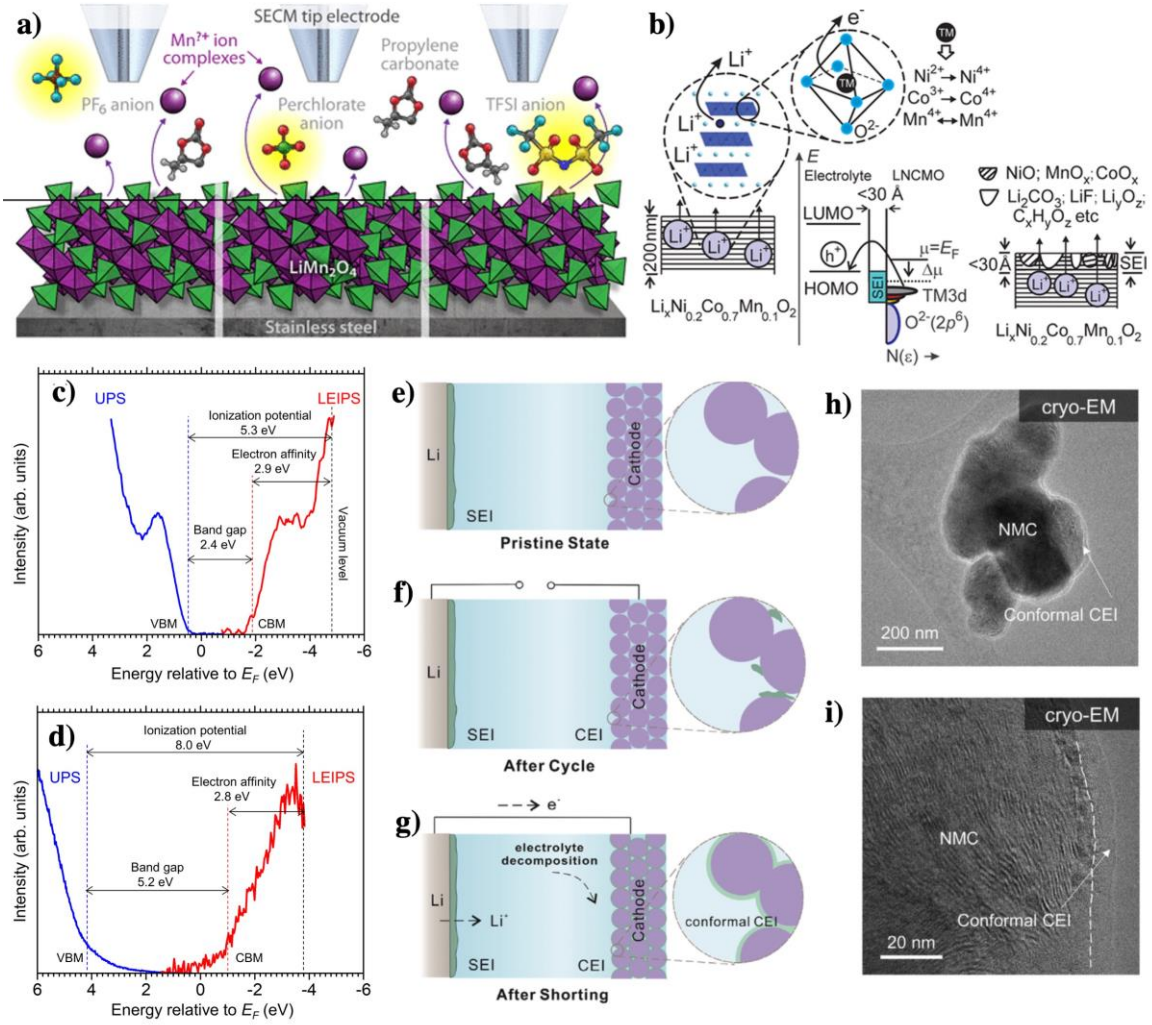

Figure 4. (a) Schematic illustration representing the interaction of $LiMn_2O_4$ with electrolyte solvent (PC), salt anions (ClO_4^-, PF_6^-, and $(CF_3SO_2)_2N^-$), and the dissolution of Mn^{2+} ions. The Schematic also depicts the *in-situ* analysis of degradation products by scanning electro-chemical microscopy (SECM) technique. Reproduced with permission.[73] Copyright 2021, American Chemical Society. (b) Schematic showing various electronic transitions during delithiation at the cathode. Delithiation is accompanied by electron loss and oxidation of the host material. Reproduced with permission.[74] Copyright 2015, American Chemical Society. (c, d) Energy diagrams of $LiCoO_2$ cathode and solid electrolyte, lithium phosphorous oxy-nitride (LiPON), obtained from ultraviolet photoelectron spectroscopy (UPS) and low-energy inverse photoelectron spectroscopy (LEIPS) analysis. Reproduced with permission.[75] Copyright 2021, American Vacuum Society. Schematic representation of CEI formation under various conditions in a LIB: (e) pristine cell, (f) cell after cycling, (g) conformal CEI formation after shorting the cell. (h, i) Cryogenic electron microscopy images of the surface of NMC

cathode showing the formation of conformal CEI at various resolutions. Reproduced with permission.[16] Copyright 2021, Elsevier.

In-situ Fourier-transform infrared (FTIR) spectroscopy has also been used to study the CEI in a LIB. The oxidation properties of propylene carbonate (PC) with $LiClO_4$ could be well-demonstrated in a $LiCoO_2$ electrode.[76] The stability and reflectivity of the film can enable the demonstration of high-quality subtractive normalized interfacial FTIR (SNIFTIR) spectra, which can detect the electrochemical oxidation reactions of non-aqueous electrolytes on the active material's surface. The FTIR studies can be complemented with *in-situ* Raman spectroscopy, which can provide information on the chemical species and composition of the CEI as well.

Charge transfer resistance at the CEI is critical for determining the power density in a battery. Based on the physicochemical aspects and evolution of the occupied and unoccupied density of states of different band spectra, the Li^+ diffusion pathways can be significantly influenced. *In-situ* analysis can monitor the real-time CEI growth; thereby, CEI's composition, morphology, stability, and thickness can be characterized.[77–79] *In-situ* synchrotron X-ray photoelectron spectroscopy (SXPS) has been introduced to study one such thin CEI film of $Li_xNi_{0.2}Co_{0.7}Mn_{0.1}O_2$.[74] It has been demonstrated that upon deintercalation of Li^+ ions, the change in Fermi level could be observed, accompanied by oxidation of Ni^{2+} and Co^{3+} ions for compensation of bulk's charge, as depicted in **Figure 4b**. Due to low-lying energy levels, a thin interface thickness of <30 Å at the $Li_{x\leq1.0}Ni_{0.2}Co_{0.7}Mn_{0.1}O_2$ electrode could be achieved, however, it leads to distortion of architecture and reduction of transition metal ions. The oxidative reactions at the interface are expected to be responsible for the complexity of the degradation mechanism. Hence, the highly oxidative nature of Ni^{2+} and Co^{3+} ions can be well-considered and should be studied to achieve a stable high-power-density Li-based material.

Likewise, synchrotron X-ray diffraction (SXRD) is vital in examining bulk and surface morphology deviation.[80] In addition, it is useful in depicting the simultaneous removal of oxygen and lithium upon charging at specific voltage plateaus. X-ray absorption spectroscopy (XAS) can support this viewpoint, which studies the structural rearrangement delivering the migration of cations from a transition metal to lithium sites. From the shape of XAS and X-ray

absorption near-edge structure (XANES) spectra, the changes in the modification of local and electronic structures are predicted. XAS analysis revealed the partial reduction of Mn ions in the discharge state. The tetravalent Mn ions were reduced to the trivalent state, which contributed to the reconstruction of the Fermi level.

Detailed characterization techniques are crucial to understand the interfacial chemical properties and information on different energy levels. Such powerful techniques include, but are not limited to, X-ray photoelectron spectroscopy (XPS), time-of-flight secondary ion mass spectrometry (TOF-SIMS), ultraviolet photoelectron spectroscopy (UPS)/low-energy inverse photoelectron spectroscopy (LEIPS). A combination of these techniques were used to study an interlayer generated between lithium phosphorous oxy-nitride (LiPON) solid electrolyte and $LiCoO_2$, caused by temperature rise.[75] The temperature elevation could change the structure of network in LiPON and incorporation of oxygen from the cathode, resulting in reduction of cobalt. The diffusion of electrons between the solid electrolyte and the electrode prompted the reduction of $LiCoO_2$, which can eventually result in decomposition of cathode. As a comparison, UPS/LEIPS spectra of LIPON and $LiCoO_2$ are shown in **Figure 4c, d** with different band gap energies.

The direct visualization of CEI with dual function of high atomic resolution and chemical characterization is of vital importance and is expected to be capable of revealing the functions of a complex CEI. Cryogenic electron microscopy, upon brief electrical shorting between the positive and negative electrodes, shows possibility of forming an *in-situ* conformal stable layer of CEI [16]. It is to note that the shorting process should be brief enough, resulting in a possibility of a controlled reduction kinetics and thus, decomposition of electrolyte happens quicker to give rise to a conformal film (see **Figure 4e-g**). As such, a uniform passivation layer can be formed at the CEI, thus suppressing undesirable reactions and providing ion conductive pathways (**Figure 4h, i**). Cryogenic electron microscopy opens a new dimension of investigating the sensitive interfacial chemistry and direct imaging at the same time, while preserving the native state of the CEI.

The various cathode and electrolyte systems and their respective CEI compositions described in this review are summarized in **Table 1**.

Table 1. A comprehensive assessment of potential cathode-electrolyte systems to stabilize the CEI.

Cathode system	**Electrolyte engineering**	**CEI composition**
$LiNi_{0.6}Mn_{0.2}Co_{0.2}O_2$ (NMC 622)[39]	Lithium difluoro(oxalato)borate (LiDFOB) or 3-hexylthiophene (3HT) additives & $LiPF_6$ in ethylene carbonate (EC)-ethyl methyl carbonate (EMC)	Stable acyl radical species, dimers
$LiCoO_2$[40]	Trimethyl borate (TMB) additive & $LiPF_6$ in ethylene carbonate/dimethyl carbonate (EC/DMC)	LiF, Li-O, lithium boron oxide (LBO) and species containing B-O, B-O-B and B-F bonds
$LiNi_{0.5}Mn_{1.5}O_4$ (LNMO)[41]	Methylboronic acid MIDA ester & $LiPF_6$ in ethylene carbonate/dimethyl carbonate (EC/DMC)	Carbonate groups (C-O), B-O, B-F, $Li_xPO_yF_z$ and less LiF compound species
$LiNi_{0.85}Co_{0.1}Mn_{0.05}O_2$ (NCM851005)[43]	Methoxytriethyleneoxypropyltrimethoxysilane (MTE-TMS) & $LiPF_6$ in ethylene carbonate/diethyl carbonate (EC/DEC)	LiF, Li_xPF_y, $Li_xPF_yO_z$ and Li_2CO_3
$LiCoO_2$[81]	Di(methylsulfonyl) ethane (DMSE) & $LiPF_6$ in the EC, dimethyl carbonate (DMC), and EMC mixed solvents	LiF, Li_xPF_y, and Li_xPOF_y
"$AlPO_4$"-coated $LiCoO_2$[58]	$LiPF_6$ in ethylene carbonate/dimethyl carbonate (EC/DMC)	Co-containing and Al-containing fluorides and/or oxyfluorides, $PF_x(OH)_y$, Li

		F and $Li_xPF_yO_z$
Aromatic polyamide (APA) coated $Li_{1.2}Mn_{0.55}Ni_{0.15}Co_{0.1}O_2$ (LMR)[57]	$LiPF_6$ in diethyl carbonate (DEC)/ ethyl methyl carbonate (EMC)/ ethylene carbonate (EC)	Aromatic polyamide, Li_2CO_3, LiF and C–O, C=O, and P-containing species
5 % and 20 % Al in $LiNi_{0.8}Co_{0.2-y}Al_yO_2$[67]	$LiPF_6$ or $LiBF_4$ in ethylene carbonate/dimethyl carbonate (EC/DMC)	Ni-F, P-O-F, and Al-O-F surface species and Al-F like species
2 at% Al in $LiNi_{0.94}Co_{0.06}O_2$ (NC) $[LiNi_{0.92}Co_{0.06}Al_{0.02}O_2]$[68]	$LiPF_6$ in ethylene carbonate/ethyl methyl carbonate (EC:EMC) with 2 wt.% vinylene carbonate	Al_2O_3 nano-islands and P-containing species
Zr^{4+}/Al^{3+} co-doped in $LiNi_{0.83}Co_{0.11}Mn_{0.06}O_2$[69]	$LiPF_6$ in ethylene carbonate/dimethyl carbonate (EC/DMC)	Zr–O and Al–O bonded species
$Li_{1-x}CoO_2$[70]	$LiBF_4$ in propylene carbonate (PC)	Polymeric film
$LiMn_2O_4$[71]	Water-in-bisalt" electrolyte (lithium bis(trifluoromethanesulfonyl)imide (LiTFSI) & lithium trifluoromethanesulfonate (LiTOf)) H_2O) with Potassium ferricyanide ($K_3Fe(CN)_6$) as redox mediator and KCl	$–(CF)_n–$ species and trace amounts of Li_2CO_3, MnF_2 and LiF.
$LiMn_2O_4$[73]	$LiPF_6$ in ethylene carbonate/dimethyl carbonate (EC/DMC)	LiF, HF and ClO_4-based products
$LiCoO_2$[76]	$LiClO_4$ in propylene carbonate	Carboxylic groups and carboxylic acid anhydrides

		group compounds
Nickel manganese cobalt oxide (NMC532)[38]	Lithium hexafluorophosphate in ethylene carbonate/diethyl carbonate (EC/DEC)	Organic polymeric composition of alkyl carbonates species, namely poly vinylene carbonate
$Li_{x\leq1.0}Ni_{0.2}Co_{0.7}Mn_{0.1}O_2$[74]	$LiPF_6$ in ethylene carbonate/dimethyl carbonate (EC/DMC)	Lithium oxides, fluorides, and carbonates
$Li_xCo_{0.13}Ni_{0.13}Mn_{0.54}O_{2-\delta}$ composite[80]	$LiPF_6$ in ethylene carbonate/dimethyl carbonate (EC/DMC)	LiO_2, Li_2O, Li_2O_2, Li_2CO_3, and lithium alkyl carbonate
$LiCoO_2$[75]	Lithium phosphorous oxy-nitride (LiPON)	Li-O, Li-O-P, Li-Co-O containing species

4. Future outlook

With the rapid advancement in high-energy metal-based batteries, interface behavior constitutes an increasingly significant challenge.[82] While there is an approximated and general understanding of the elemental composition of the interfacial film between cathode and electrolyte, establishing a solid perception of the mechanism and function of a CEI is critical for enhancing the performance of batteries. To this end, multiple prospects can be applied in interfacial engineering towards achieving a practical high-performance battery. Trailblazing innovations have come to light from research on the SEI,[83–85] and it is expected that the following approaches can bring about optimal results towards interfacial engineering of the CEI as well.

i) Advanced characterization techniques

Understanding the CEI's formation and evolution mechanisms via various advanced operando characterization tools is imperative to gain further insights. Liquid-phase transmission electron microscopy (LP-TEM) is one of such powerful characterization techniques to understand the importance of failure mechanisms resulting from EEI. Right now, most of the LP-TEM studies have been devoted to studying the SEI rather than the CEI.[86,87] Based on nanometer-scale dynamics, LP-TEM can allow the probing of chemically-driven species in electrolyte environments and provide real-time analysis of SEI.[88] The electrochemical degradation of a SEI may stem from poor kinetics and chemical/electrochemical/mechanical instability, which can be due to the difference in electric potential and distribution of ionic potential gradient.[89] Note that this degradation mechanism can be mimicked by solvated high-energy electrons generated through LP-TEM, allowing observation of kinetic reaction performance at the nanometre scale level. Based on these profound findings and real-time visualization, LP-TEM is likely to contribute to understanding the CEI as well. LP-TEM can successfully provide rich-spatial experimental data with high temporal statistics. In combination with high-end computer simulations, LP-TEM can potentially provide quantitative information into multiple dynamic structures at various conditions in an effective way.[90]

Multiple reaction pathways based on XPS or UPS have been proposed earlier to analyze the important behavior of CEI films. However, many unresolved queries on CO_2 dissolution have still been unanswered. Recently, the *in-situ* surface evolution of Li-anode upon CO_2 exposure is unveiled through ambient pressure XPS (APXPS) to analyze the detrimental effects of CO_2 on the formation of the SEI.[91] This spectroscopic technique allows a detailed study of surface reactions in the presence of electrolyte, and enables an in-depth understanding of the reaction process and its intermediates involved in the pathway. *In-situ* APXPS has shed light on the new opportunities to uncover the electrochemical kinetic reactions of the SEI under realistic operating conditions.[92] Despite these, APXPS targeted method developments towards enhanced dynamic measurement conditions to enable a prerequisite interpretation of correct data for the interface studies based on probing depth.[93] Such new techniques can also be exploited to provide mechanistic insights into conditions that can favor and impede the CEI's evolution for developing a better LIB.

ii) Advanced computational models

The complex phenomena of CEI's growth mechanism and the dearth of reliable *in-situ* techniques have made it difficult to comprehend the CEI thoroughly. Current experimental techniques enable characterization of the CEI's chemical composition. Beyond that, for instance, information on the thermodynamic properties and kinetic aspects of interface properties and redox reactions is still lacking. Fortunately, various state-of-the-art computational models based on density functional theory, molecular dynamics and kinetic Monte Carlo have come to light to investigate the EEI.[94,95] Density functional tight-binding (DFTB) is one such efficient quantum model to mechanically simulate and analyze various band structures, diffusion, and reaction energies. As a result, DFTB has been found to compute electronic structures of the complex SEI interfaces accurately. Based on 2nd order charge density fluctuations of Kohn-Sham total energy, DFTB is an effective predictive modeling technique that allowed thorough investigation of the electron tunneling effect, de-solvation, facilitated ion transport, and voltage fluctuations in the SEI formed.[96]

Effective simulation methods are emerging for modeling of a higher predictive and descriptive EEI layer, such as machine learning, phase-field approach, Lagrangian method, and others.[97] For example, a machine learning-based non-linear predictive model has been used to minimize the SEI's growth in the charging phase. In particular, the single-particle model (SPM) could optimize the battery charging conditions using "orthogonal projection-based model reformulation." Besides minimizing the SEI layer, the computational algorithm guarantees an attenuated film resistance in the proposed optimal charging regime.[98] Similarly, phase-field models (PFM) could also consider the impact of SEI on the electrodeposition evolution of Li-ions. PFM has been applied to analyze the evolution of lithium filament and its bush-like morphology and its transition among them. PFM results predicted the growth of hydrostatic stresses during filament growth.[99] The highest stress values were recorded at the root of the filaments, which contributes to the instability of filaments and results in the twisting and splitting of filaments. Predictions from PFM suggested experimentalists to engineer the stress accumulation effect at the root of filaments on anodic surfaces, which can effectively suppress dendritic growth. Besides, the diffusion of Li-ions across the SEI layer could be well-monitored by adopting noise field and thus, allowing us to get a deeper insight into the SEI's redox mechanism.[99] On application of simple capacity fading model, the growth rate of SEI could be analyzed based on the decomposition rate of electrolyte species.[100] To describe the reactive transport near the EEI surface, smoothed particle hydrodynamics based on the Lagrangian simulation method were also used. At various current densities, distribution of Li-ion

deposition near the interface and determination of its nucleation and growth at the SEI could be accessed by the computational modeling.[101]

Recently, a unique 4D computational modeling (3D+time) approach is proposed, which helps reveal the heterogeneity of the SEI layer within the porous cathodes. The model could help investigate the impact of the cathode's mesostructure on the interface formation and performance of the electrode. Also, the unique distribution of SEI layers as a function of graphite electrode particles could be predicted using this novel approach. Based on the different types of graphite, it could be simulated that the spherical-type electrode showed the homogenous distribution of particles in the interface layer.[102] The possible directions proposed here for investigating SEI may be applied to CEI as well, paving the path for unveiling the synergistic mechanism of interfaces in cathode systems.

iii) Potential studies of CEI in post-LIB technologies

Since the complex CEI formation is not only confined to LIBs, CEI formation has also been reported for the post-LIB technologies. For instance, lithium-selenium (Li-Se) batteries showed the formation of a stable CEI.[103] It was analyzed that the formation of CEI with a Li-F-rich layer offered stability and conductivity at the cathode consisting of a hierarchically porous carbon sphere used to host selenium cathode. A combination of DFT calculation and XPS analysis showed that the CEI comprised of Li-F compounds. Sulfur cathode has also been employed in various metal-based batteries, such as Li-S, Na-S, and others.[104–108] It has been reported that unstable CEI in these systems can be formed, lowering the overall Coulombic efficiency and thus, promoting capacity decay.[109],[110] On the other hand, a stable CEI can be formed on sulfur-microporous carbon cathode by using fluoroethylene carbonate (FEC) additive in carbonate-based electrolytes.[111] The sulfur cathode with FEC additive showed an inorganic sodium fluoride phase in the CEI, leading to more stable battery performance, compared to the case without additive which showed an organic carbonate-based CEI. Solid-state lithium metal batteries are also often plagued with CEI formation issues.[112] The inclusion of ionic liquid could mitigate the parasitic reactions at the interface, ensuring higher oxidative stability with reduced interfacial resistance.[113]

Similarly, sodium-ion battery with layered oxide cathode also experiences parasitic reactions at the CEI. As a result, reduction of transition metal ion occurs that leads to cracks at the inter-

granular spaces.[114] As observed for LIB, the electrolyte additive approach to create artificial CEI has also been explored in a sodium-ion battery. Sodium fluoride (NaF) and sodium carbonate (Na_2CO_3) have been identified as stable compounds in the SEI layer of a sodium-ion battery.[115] Stable CEI in sodium-ion battery can be introduced by incorporating a sacrificial sodium salt, sodium mesoxalate monohydrate ($Na_2C_3O_5.H_2O$), which functioned as a cathode sodiation additive.[116] As interfaces between electrode and electrolyte govern the electrochemical performance, engineering the interfaces can significantly enhance the performance.[117,118] In recent findings, the CEI layer was probed in a sodium-ion battery delivering excellent cyclic performance and rate capability.[119] A uniformly-regulated conformal interface was found on the surface of a carbon-coated flower-shaped $Na_3V_2(PO_4)_3$/C (NVP/C) cathode. These studies may open up opportunities in understanding the interface's chemistry and their design to achieve energy- and power-dense rechargeable metal-based batteries. Particularly, visualizing the interfacial structures and their properties is crucial to realizing the future development of post-LIB cathodes.

5. Conclusion

Low electronic conductivity and high ionic conductivity are two unique attributes of an ideal CEI. Many controversies exist from various research groups regarding the resemblance of SEI with CEI. Insufficient information on the structural and chemical aspects likely results in these ambiguities. Studies that combine chemical information with in-plane spatial resolution of CEI are crucial. Several other obstructions may hinder the interpretation of these characterization techniques, such as electrolyte residue, soluble phases, complex chemistry, sensitivity to air and moisture, etc. In this regard, direct *in-situ* visualization with the dual function of high atomic resolution and chemical characterization is vital and is expected to reveal the functions of a complex CEI. To understand the formation and evolution of the interface, it is also necessary to qualitatively and quantitatively predict the formation and degradation mechanisms of the CEI through computational modelling. Building a favorable CEI requires multiple strategies according to various analytical aspects of interface mechanisms as discussed above. With substantial in-depth studies of the CEI properties, the next generation batteries with robust CEI could become a reality soon.

Acknowledgements

Sungjemmenla, C.B.S., and S.K.V. acknowledge the scholarship awarded by the Indian Institute of Technology Delhi (IIT Delhi), and University of Queensland-IIT Delhi Academy of Research (UQIDAR). Z.W.S. acknowledges the support of the Singapore National Research Foundation (NRF-NRFF2017-04) and Agency for Science, Technology and Research (Central Research Fund Award).

Author contributions

Sungjemmenla, S. K. Vineeth, Chhail Bihari Soni: Writing - original draft. Vipin Kumar, Zhi Wei Seh: Writing - review & editing.

Conflicts of interest

There are no conflicts to declare.

Reference

[1] T. Kim, W. Song, D. Y. Son, L. K. Ono, Y. Qi, *J. Mater. Chem. A* **2019**, *7*, 2942.

[2] Sungjemmenla, C. B. Soni, V. Kumar, *Nanoscale Adv.* **2021**, *3*, 1569.

[3] N. S. Jishnu, S. K. Vineeth, A. Das, N. T. M. Balakrishnan, A. P. Thomas, M. J. Jabeen Fatima, J.-H. Ahn, R. Prasanth, **2021**, 201–234.

[4] Y. Li, M. Liu, X. Feng, Y. Li, F. Wu, Y. Bai, C. Wu, *ACS Energy Lett.* **2021**, *6*, 3307.

[5] S. P. Kühn, K. Edström, M. Winter, I. Cekic-Laskovic, *Adv. Mater. Interfaces* **2022**, *9*, 2102078.

[6] S. Haber, M. Leskes, *Adv. Mater.* **2018**, *30*, 1706496.

[7] M. Gauthier, T. J. Carney, A. Grimaud, L. Giordano, N. Pour, H. H. Chang, D. P. Fenning, S. F. Lux, O. Paschos, C. Bauer, F. Maglia, S. Lupart, P. Lamp, Y. Shao-Horn, *J. Phys. Chem. Lett.* **2015**, *6*, 4653.

[8] E. Peled, S. Menkin, *J. Electrochem. Soc.* **2017**, *164*, A1703.

[9] F. M. Weber, I. Kohlhaas, E. Figgemeier, *J. Electrochem. Soc.* **2020**, *167*, 140523.

[10] S. Su, J. Ma, L. Zhao, K. Lin, Q. Li, S. Lv, F. Kang, Y. B. He, *Carbon Energy* **2021**, 1.

[11] Q. Wu, S. Mao, Z. Wang, Y. Tong, Y. Lu, *Nano Sel.* **2020**, *1*, 111.

[12] R. Hausbrand, D. Becker, W. Jaegermann, *Prog. Solid State Chem.* **2014**, *42*, 175.

[13] H. Wang, X. Li, F. Li, X. Liu, S. Yang, J. Ma, *Electrochem. commun.* **2021**, *122*, 106870.

[14] K. Nie, Y. Hong, J. Qiu, Q. Li, X. Yu, H. Li, L. Chen, *Front. Chem.* **2018**, *6*, 1.

[15] S. N. Steinmann, Z. W. Seh, *Nat. Rev. Mater.* **2021**, *6*, 289.

[16] Z. Zhang, J. Yang, W. Huang, H. Wang, W. Zhou, Y. Li, Y. Li, J. Xu, W. Huang, W. Chiu, Y. Cui, *Matter* **2021**, *4*, 302.

[17] G. Zampardi, F. La Mantia, *Batter. Supercaps* **2020**, *3*, 672.

[18] Y. Xie, H. Gao, J. Gim, A. T. Ngo, Z. F. Ma, Z. Chen, *J. Phys. Chem. Lett.* **2019**, *10*, 589.

[19] Y. Lu, X. Zhang, C. Xue, C. Xin, M. Li, C. Nan, Y. Shen, *Mater. Today Energy* **2020**, *18*, 100522.

[20] D. Bosubabu, J. Sivaraj, R. Sampathkumar, K. Ramesha, *ACS Appl. Energy Mater.* **2019**, *2*, 4118.

[21] W. P. Wang, J. Zhang, J. Chou, Y. X. Yin, Y. You, S. Xin, Y. G. Guo, *Adv. Energy Mater.* **2021**, *11*, 1.

[22] Z. Hu, S. Zhang, S. Dong, Q. Li, G. Cui, L. Chen, *Chem. Mater.* **2018**, *30*, 4039.

[23] H. Maleki Kheimeh Sari, X. Li, *Adv. Energy Mater.* **2019**, *9*, 1.

[24] P. Verma, P. Maire, P. Novák, *Electrochim. Acta* **2010**, *55*, 6332.

[25] R. V. Gadhave, S. K. Vineeth, P. A. Mahanwar, P. T. Gadekar, *J. Adhes. Sci. Technol.* **2021**, *35*, 1072.

[26] I. Takahashi, H. Kiuchi, A. Ohma, T. Fukunaga, E. Matsubara, *J. Phys. Chem. C* **2020**, *124*, 9243.

[27] H. Maleki Kheimeh Sari, X. Li, *Adv. Energy Mater.* **2019**, *9*, 1970151.

[28] S. K. Vineeth, C. B. Soni, Y. Sun, V. Kumar, Z. W. Seh, *Trends Chem.* **2022**, *4*, 48.

[29] X. Chen, N. Yao, B.-S. Zeng, Q. Zhang, *Fundam. Res.* **2021**, *1*, 393.

[30] D. Zhao, S. Li, *Front. Chem.* **2020**, *8*, 1.

[31] X. Shi, T. Zheng, J. Xiong, B. Zhu, Y. Cheng, Y. Xia, *ACS Appl. Mater. Interfaces* **2021**, *13*, 57107.

[32] X. Yu, A. Manthiram, *Energy Environ. Sci.* **2018**, *11*, 527.

[33] J. P. Robinson, P. D. Kichambare, J. L. Deiner, R. Miller, M. A. Rottmayer, G. M. Koenig, *J. Am. Ceram. Soc.* **2018**, *101*, 1087.

[34] F. Cheng, X. Zhang, Y. Qiu, J. Zhang, Y. Liu, P. Wei, M. Ou, S. Sun, Y. Xu, Q. Li, C. Fang, J. Han, Y. Huang, *Nano Energy* **2021**, *88*, 106301.

[35] P. Jankowski, W. Wieczorek, P. Johansson, *J. Mol. Model.* **2017**, *23*.

[36] R. W. Schmitz, P. Murmann, R. Schmitz, R. Müller, L. Krämer, J. Kasnatscheew, P. Isken, P. Niehoff, S. Nowak, G. V. Röschenthaler, N. Ignatiev, P. Sartori, S. Passerini, M. Kunze, A. Lex-Balducci, C. Schreiner, I. Cekic-Laskovic, M. Winter, *Prog. Solid State Chem.* **2014**, *42*, 65.

[37] S. S. Zhang, *J. Power Sources* **2006**, *162*, 1379.

[38] M. Hekmatfar, I. Hasa, R. Eghbal, D. V. Carvalho, A. Moretti, S. Passerini, *Adv. Mater. Interfaces* **2020**, *7*, 1.

[39] H. Gao, F. Maglia, P. Lamp, K. Amine, Z. Chen, *ACS Appl. Mater. Interfaces* **2017**, *9*, 44542.

[40] Q. Liu, G. Yang, S. Liu, M. Han, Z. Wang, L. Chen, *ACS Appl. Mater. Interfaces* **2019**, *11*, 17435.

[41] Y.-Q. Chen, T.-Y. Chen, W.-D. Hsu, T.-Y. Pan, L.-J. Her, W.-M. Chang, M.

Wohlfahrt-Mehrens, H. Yoshitake, C.-C. Chang, *J. Power Sources* **2020**, *477*, 228473.

[42] X. T. Wang, Z. Y. Gu, W. H. Li, X. X. Zhao, J. Z. Guo, K. Di Du, X. X. Luo, X. L. Wu, *Chem. - An Asian J.* **2020**, *15*, 2803.

[43] H. Q. Pham, M. Mirolo, M. Tarik, M. El Kazzi, S. Trabesinger, *Energy Storage Mater.* **2020**, *33*, 216.

[44] L. Droguet, G. M. Hobold, M. F. Lagadec, R. Guo, C. Lethien, M. Hallot, O. Fontaine, J. M. Tarascon, B. M. Gallant, A. Grimaud, *ACS Energy Lett.* **2021**, *6*, 2575.

[45] W. Luo, C. F. Lin, O. Zhao, M. Noked, Y. Zhang, G. W. Rubloff, L. Hu, *Adv. Energy Mater.* **2017**, *7*, 1.

[46] X. Xiao, P. Lu, D. Ahn, *Adv. Mater.* **2011**, *23*, 3911.

[47] T. Feng, Y. Xu, Z. Zhang, X. Du, X. Sun, L. Xiong, R. Rodriguez, R. Holze, *ACS Appl. Mater. Interfaces* **2016**, *8*, 6512.

[48] B. Kim, J. G. Lee, M. Choi, J. Cho, B. Park, *J. Power Sources* **2004**, *126*, 190.

[49] J. Kim, M. Noh, J. Cho, H. Kim, K.-B. Kim, *J. Electrochem. Soc.* **2005**, *152*, A1142.

[50] Y. J. Kim, J. Cho, T.-J. Kim, B. Park, *J. Electrochem. Soc.* **2003**, *150*, A1723.

[51] J. Cho, T.-G. Kim, C. Kim, J.-G. Lee, Y.-W. Kim, B. Park, *J. Power Sources* **2005**, *146*, 58.

[52] G. T.-K. Fey, C.-Z. Lu, J.-D. Huang, T. P. Kumar, Y.-C. Chang, *J. Power Sources* **2005**, *146*, 65.

[53] S. Oh, J. K. Lee, D. Byun, W. I. Cho, B. Won Cho, *J. Power Sources* **2004**, *132*, 249.

[54] Y. K. Sun, S. W. Cho, S. T. Myung, K. Amine, J. Prakash, *Electrochim. Acta* **2007**, *53*, 1013.

[55] S. Chen, L. Shen, P. A. van Aken, J. Maier, Y. Yu, *Adv. Mater.* **2017**, *29*.

[56] Q. Zhang, L. Han, J. Pan, Z. Chen, Y. T. Cheng, *Appl. Phys. Lett.* **2017**, *110*, 1.

[57] C. Ye, Y. Qiu, X. Luo, M. Chen, Y. Zhong, B. Wu, L. Xing, Y. Liao, W. Li, *Chem. Eng. J.* **2021**, *403*, 126366.

[58] Y. C. Lu, A. N. Mansour, N. Yabuuchi, Y. Shao-Horn, *Chem. Mater.* **2009**, *21*, 4408.

[59] M. Schnabel, E. Arca, Y. Ha, C. Stetson, G. Teeter, S. D. Han, P. Stradins, *ACS Appl. Energy Mater.* **2020**, *3*, 8842.

[60] X. Jin, Q. Xu, H. Liu, X. Yuan, Y. Xia, *Electrochim. Acta* **2014**, *136*, 19.

[61] P. K. Nayak, J. Grinblat, M. Levi, O. Haik, E. Levi, D. Aurbach, *J. Solid State Electrochem.* **2015**, *19*, 2781.

[62] D. Wang, Y. Huang, Z. Huo, L. Chen, *Electrochim. Acta* **2013**, *107*, 461.

[63] Q. Li, G. Li, C. Fu, D. Luo, J. Fan, L. Li, *ACS Appl. Mater. Interfaces* **2014**, *6*, 10330.

[64] P. K. Nayak, J. Grinblat, M. Levi, E. Levi, S. Kim, J. W. Choi, D. Aurbach, *Adv. Energy Mater.* **2016**, *6*, 1.

[65] W. Li, X. Liu, H. Celio, P. Smith, A. Dolocan, M. Chi, A. Manthiram, *Adv. Energy Mater.* **2018**, *8*, 1.

[66] M. Dixit, B. Markovsky, D. Aurbach, D. T. Major, *J. Electrochem. Soc.* **2017**, *164*, A6359.

[67] Z. W. Lebens-Higgins, D. M. Halat, N. V. Faenza, M. J. Wahila, M. Mascheck, T. Wiell, S. K. Eriksson, P. Palmgren, J. Rodriguez, F. Badway, N. Pereira, G. G. Amatucci, T. L. Lee, C. P. Grey, L. F. J. Piper, *Sci. Rep.* **2019**, *9*, 1.

[68] L. Zou, J. Li, Z. Liu, G. Wang, A. Manthiram, C. Wang, *Nat. Commun.* **2019**, *10*, 3447.

[69] Z. Zhu, Y. Liang, H. Hu, A. Gao, T. Meng, D. Shu, F. Yi, J. Ling, *J. Power Sources* **2021**, *498*, 229857.

[70] M. G. S. R. Thomas, P. G. Bruce, J. B. Goodenough, *J. Electrochem. Soc.* **1985**, *132*, 1521.

[71] S. Liu, D. Liu, S. Wang, X. Cai, K. Qian, F. Kang, B. Li, *J. Mater. Chem. A* **2019**, *7*, 12993.

[72] P. K. Nayak, E. M. Erickson, F. Schipper, T. R. Penki, N. Munichandraiah, P. Adelhelm, H. Sclar, F. Amalraj, B. Markovsky, D. Aurbach, *Adv. Energy Mater.* **2018**,

8, 1.

[73] D. Huang, C. Engtrakul, S. Nanayakkara, D. W. Mulder, S. D. Han, M. Zhou, H. Luo, R. C. Tenent, *ACS Appl. Mater. Interfaces* **2021**, *13*, 11930.

[74] G. Cherkashinin, M. Motzko, N. Schulz, T. Späth, W. Jaegermann, *Chem. Mater.* **2015**, *27*, 2875.

[75] S. Iida, M. Terashima, K. Mamiya, H.-Y. Chang, S. Sasaki, A. Ono, T. Kimoto, T. Miyayama, *J. Vac. Sci. Technol. B* **2021**, *39*, 044001.

[76] K. Kanamura, S. Toriyama, S. Shiraishi, M. Ohashi, Z. Takehara, *J. Electroanal. Chem.* **1996**, *419*, 77.

[77] S. Wenzel, T. Leichtweiss, D. A. Weber, J. Sann, W. G. Zeier, J. Janek, *ACS Appl. Mater. Interfaces* **2016**, *8*, 28216.

[78] M. Yan, W.-P. Wang, Y.-X. Yin, L.-J. Wan, Y.-G. Guo, *EnergyChem* **2019**, *1*, 100002.

[79] S.-K. Jung, H. Gwon, S.-S. Lee, H. Kim, J. C. Lee, J. G. Chung, S. Y. Park, Y. Aihara, D. Im, *J. Mater. Chem. A* **2019**, *7*, 22967.

[80] N. Yabuuchi, K. Yoshii, S. T. Myung, I. Nakai, S. Komaba, *J. Am. Chem. Soc.* **2011**, *133*, 4404.

[81] X. Zheng, T. Huang, G. Fang, Y. Pan, Q. Li, M. Wu, *ACS Appl. Mater. Interfaces* **2019**, *11*, 36244.

[82] D. Aurbach, *J. Power Sources* **2000**, *89*, 206.

[83] B. Horstmann, F. Single, A. Latz, *Curr. Opin. Electrochem.* **2019**, *13*, 61.

[84] V. A. Agubra, J. W. Fergus, *J. Power Sources* **2014**, *268*, 153.

[85] J. Kim, O. B. Chae, B. L. Lucht, *J. Electrochem. Soc.* **2021**, *168*, 030521.

[86] Z. Ahmad, V. Venturi, H. Hafiz, V. Viswanathan, *J. Phys. Chem. C* **2021**, *125*, 11301.

[87] C. B. Soni, V. Kumar, Z. W. Seh, *Batter. Supercaps* **2022**, *5*, e202100207. doi:10.1002/batt.202100207

[88] S. M. Rehn, M. R. Jones, *ACS Energy Lett.* **2018**, *3*, 1269.

[89] C. B. Soni, Sungjemmenla, S. K. Vineeth, V. Kumar, *Energy Storage* **2022**, *4*, e264. doi:10.1002/est2.264

[90] C. Z. Zhao, B. C. Zhao, C. Yan, X. Q. Zhang, J. Q. Huang, Y. Mo, X. Xu, H. Li, Q. Zhang, *Energy Storage Mater.* **2020**, *24*, 75.

[91] A. Etxebarria, A. Etxebarria, D. J. Yun, D. J. Yun, M. Blum, M. Blum, Y. Ye, Y. Ye, Y. Ye, M. Sun, K. J. Lee, K. J. Lee, H. Su, H. Su, M. Á. Muñoz-Márquez, P. N. Ross, E. J. Crumlin, E. J. Crumlin, *ACS Appl. Mater. Interfaces* **2020**, *12*, 26607.

[92] Y. C. Lu, E. J. Crumlin, G. M. Veith, J. R. Harding, E. Mutoro, L. Baggetto, N. J. Dudney, Z. Liu, Y. Shao-Horn, *Sci. Rep.* **2012**, *2*, 1.

[93] J. Maibach, I. Källquist, M. Andersson, S. Urpelainen, K. Edström, H. Rensmo, H. Siegbahn, M. Hahlin, *Nat. Commun.* **2019**, *10*, 1.

[94] A. A. Franco, A. Rucci, D. Brandell, C. Frayret, M. Gaberscek, P. Jankowski, P. Johansson, *Chem. Rev.* **2019**, *119*, 4569.

[95] A. Yong, S. Eng, C. B. Soni, Y. Lum, E. Khoo, Z. Yao, S. K. Vineeth, V. Kumar, J. Lu, C. S. Johnson, **2022**, *2422*.

[96] Y. Li, K. Leung, Y. Qi, *Acc. Chem. Res.* **2016**, *49*, 2363.

[97] A. Wang, S. Kadam, H. Li, S. Shi, Y. Qi, *npj Comput. Mater.* **2018**, *4*.

[98] M. S. S. Malik, G. Li, Z. Chen, *J. Power Sources* **2021**, *482*.

[99] V. Yurkiv, T. Foroozan, A. Ramasubramanian, R. Shahbazian-Yassar, F. Mashayek, *Electrochim. Acta* **2018**, *265*, 609.

[100] E. M. Perassi, E. P. M. Leiva, *Electrochim. Acta* **2019**, *308*, 418.

[101] K. Dong, Y. Xu, J. Tan, M. Osenberg, F. Sun, Z. Kochovski, D. T. Pham, S. Mei, A. Hilger, E. Ryan, Y. Lu, J. Banhart, I. Manke, *ACS Energy Lett.* **2021**, *6*, 1719.

[102] M. Chouchane, O. Arcelus, A. A. Franco, *Batter. Supercaps* **2021**, *4*, 1457.

[103] Z.-P. Zhuang, X. Dai, W.-D. Dong, L.-Q. Jiang, L. Wang, C.-F. Li, J.-X. Yang, L. Wu,

Z.-Y. Hu, J. Liu, L.-H. Chen, Y. Li, B.-L. Su, *Electrochim. Acta* **2021**, *393*, 139042.

[104] Sungjemmenla, C. B. Soni, S. K. Vineeth, V. Kumar, *Mater. Adv.* **2021**, *2*, 4165.

[105] Sungjemmenla, C. B. Soni, S. K. Vineeth, V. Kumar, *Adv. Energy Sustain. Res.* **2021**, 2100157. doi:10.1002/aesr.202100157

[106] V. Kumar, Y. Wang, A. Y. S. Eng, M. F. Ng, Z. W. Seh, *Cell Reports Phys. Sci.* **2020**, *1*, 100044.

[107] Z. W. Seh, Y. Sun, Q. Zhang, Y. Cui, *Chem. Soc. Rev.* **2016**, *45*, 5605.

[108] A. Y. S. Eng, V. Kumar, Y. Zhang, J. Luo, W. Wang, Y. Sun, W. Li, Z. W. Seh, *Adv. Energy Mater.* **2021**, *11*, 1.

[109] W. Wang, J. Zhang, J. Chou, Y. Yin, Y. You, S. Xin, Y. Guo, *Adv. Energy Mater.* **2021**, *11*, 2000791.

[110] X. Xing, Y. Li, X. Wang, V. Petrova, H. Liu, P. Liu, *Energy Storage Mater.* **2019**, *21*, 474.

[111] A. Y. S. Eng, Y. Wang, D. T. Nguyen, S. Y. Tee, C. Y. J. Lim, X. Y. Tan, M. F. Ng, J. Xu, Z. W. Seh, *Nano Lett.* **2021**, *21*, 5401.

[112] Y. Xiao, Y. Wang, S. H. Bo, J. C. Kim, L. J. Miara, G. Ceder, *Nat. Rev. Mater.* **2020**, *5*, 105.

[113] Q. Zhang, K. Pan, M. Jia, X. Zhang, L. Zhang, H. Zhang, S. Zhang, *Electrochim. Acta* **2021**, *368*, 137593.

[114] L. Mu, X. Feng, R. Kou, Y. Zhang, H. Guo, C. Tian, C. Sun, X. Du, D. Nordlund, H. L. Xin, F. Lin, *Adv. Energy Mater.* **2018**, *8*, 1801975.

[115] G. G. Eshetu, T. Diemant, M. Hekmatfar, S. Grugeon, R. J. Behm, S. Laruelle, M. Armand, S. Passerini, *Nano Energy* **2019**, *55*, 327.

[116] A. J. Fernández-Ropero, M. Zarrabeitia, G. Baraldi, M. Echeverria, T. Rojo, M. Armand, D. Shanmukaraj, *ACS Appl. Mater. Interfaces* **2021**, *13*, 11814.

[117] J. Song, B. Xiao, Y. Lin, K. Xu, X. Li, *Adv. Energy Mater.* **2018**, *8*, 1703082.

[118] K. Chen, K. Yamamoto, Y. Orikasa, T. Uchiyama, Y. Ito, S. Yubuchi, A. Hayashi, M. Tatsumisago, K. Nitta, T. Uruga, Y. Uchimoto, *Solid State Ionics* **2018**, *327*, 150.

[119] M. Ihsan-Ul-Haq, J. Cui, N. Mubarak, M. Xu, X. Shen, Z. Luo, B. Huang, J.-K. Kim, *Adv. Energy Sustain. Res.* **2021**, *2*, 2100072.